Application of Voltammetric Techniques at Microelectrodes to the Study of the Chemical Stability of Highly Reactive Species

E. Laborda, J. M. Olmos, E. Torralba, A. Molina*

Departamento de Química Física, Facultad de Química, Regional Campus of International Excellence "Campus Mare Nostrum", Universidad de Murcia, 30100 Murcia, Spain

* Corresponding author:

Tel: +34 868 88 7524

Fax: +34 868 88 4148

Email: amolina@um.es

Abstract

The application of voltammetric techniques to the study of chemical speciation and stability is addressed both theoretically and experimentally in this work. In such systems, electrode reactions are coupled to homogeneous chemical equilibria (complexations, protonations, ion associations,…) that can be studied in a simple, economical and accurate way by means of electrochemical methods. These are of particular interest when some of the participating species are unstable given that the generation and characterization of the species are performed *in situ* and in a short time scale.

With the above aim, simple explicit solutions are presented in this paper for quantitative characterization with any voltammetric technique and with the most common electrode geometries. From the theoretical results obtained, it is pointed out that the use of square wave voltammetry in combination with microelectrodes is very suitable. Finally, the theory is applied to the investigation of the ion association between the anthraquinone radical monoanion and the tetrabutylammonium cation in acetonitrile medium.

Keywords: Chemical speciation; Microelectrode; Cyclic voltammetry; Square wave voltammetry; Anthraquinone radical anion

1. INTRODUCTION

In many electrochemical systems the electron transfer of organic and inorganic compounds is coupled to homogeneous chemical processes [1, 2]. These affect the electrochemical response so that the chemical behavior and properties of the species can be studied by means of electrochemical methods. These techniques are very advantageous given that the instrumentation is economical, portable and relatively simple, and *in situ* studies can be performed without complex sample preparation and in a short period time.

Scheme I corresponds to the general situation where species A is electroreduced to B and both species, A and B, take part in a number of chemical equilibria in solution the products of which (AL, BL, … AL_n, BL_n) are also electroactive:

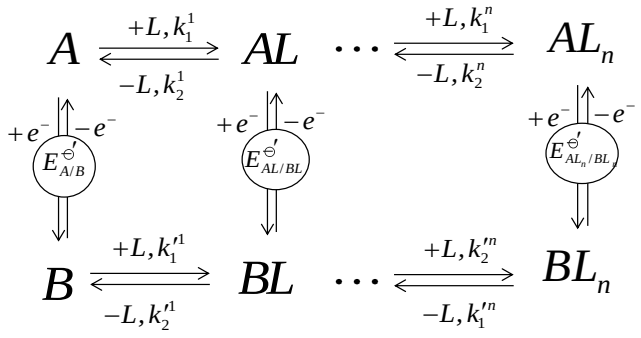

Scheme I

Species L is assumed to be present at high concentration $\left(c_L^* >> c_A^*, c_B^*, c_{AL_i}^*, c_{BL_i}^*\right)$ and k_j^i and $k_j'^i$ (j=1, 2 ; i=1, 2...n) represent the (pseudo)first-order forward and backward rate constants of the chemical reactions. Note that this scheme allows for the study of different common mechanisms by simply adjusting the values of the equilibrium constants. Thus, the situation where only the oxidized (A) or the reduced (B) species is involved in the homogeneous chemical equilibria (i.e. only one species reacts in solution) can be studied by setting to zero the formation equilibrium constant(s) of the other species (that is, the C_n^{eq} E^{rev} or E^{rev} C_n^{eq} – type mechanisms). Note that the

$E^{rev}\ C_n^{eq}$ mechanism is very usual in real systems given that the electron transfer generally decreases the stability of the chemical species, for example, when radicals are formed.

In this paper, the voltammetric study of Scheme I is carried out both theoretically and experimentally. In the first part of the paper, a simple explicit solution is derived valid for any voltammetric technique (including the widely-used cyclic (CV) and square wave voltammetries (SWV)) at microelectrodes of various geometries. From the theoretical solutions, the influence of the chemical equilibria as well as that of the electrode size and geometry on the voltammetric response is analyzed in CV and SWV. As a result, the optimum conditions and voltammetric technique for quantitative speciation studies are discussed, the use of microelectrodes in conjunction with square wave voltammetry being recommended. This technique is advantageous over cyclic voltammetry since the ohmic drop and background effects are greatly reduced (due to the differential nature of SWV) and the voltammograms always show a peak shape so that the determination of the position is easier and more accurate than in CV, which yields sigmoid responses when the electrode size is decreased. Moreover, the peak potentials are not a function of the electrode geometry so that errors in its determination do not affect the results. Also, methods to detect the presence of chemical equilibria coupled to the electron transfer and to determine the equilibrium constants and standard potentials are proposed.

The theory is applied to the experimental investigation of the ion pairing between the radical anion $AQ^{\bullet-}$ originated by the electroreduction of anthraquinone (AQ) and the cation tetrabutylammonium (NBu_4^+) in acetonitrile medium. The global process proceeds via the $E^{rev}\ C^{eq}$ mechanism where the reduced species is the radical monoanion. The characterization of this species, and in general of radicals, is important

in the fields of chemistry and biochemistry since they participate in processes of great interest in biomedical science, industrial synthesis and electrochemical technologies [3-5]. Among them, it is worth mentioning the key role of $AQ^{\bullet-}$ in the catalysis of oxygen electroreduction for H_2O_2 production [3, 6-8].

2. THEORY

2.1 *Application of a constant potential pulse*

Let us consider the reversible electroreduction of species A which is affected by a series of complexation reactions according to Scheme I, being $E^{\ominus'}_{\mathrm{A/B}}$ and $E^{\ominus'}_{\mathrm{AL_i/BL_i}}$ the formal potentials of the redox couples $\mathrm{A/B}$ and $\mathrm{AL}_i/\mathrm{BL}_i$, respectively.

When a constant potential, *E*, is applied to the working electrode immersed in the solution containing species A and L such that electron transfer reactions take place, the mass transport supposed by purely diffusion is described by the following differential diffusive-kinetic equation system:

$$\left.\begin{aligned}
\frac{\partial c_{\mathrm{AL_i}}}{\partial t} &= D_{\mathrm{AL_i}}\nabla^2 c_{\mathrm{AL_i}} + k_1{}^{i} c_{\mathrm{AL_{i-1}}} - (k_2{}^{i} + k_1{}^{i+1}) c_{\mathrm{AL_i}} + k_2{}^{i+1} c_{\mathrm{AL_{i+1}}} \\
\frac{\partial c_{\mathrm{BL_i}}}{\partial t} &= D_{\mathrm{BL_i}}\nabla^2 c_{\mathrm{BL_i}} + k'_1{}^{i} c_{\mathrm{BL_{i-1}}} - (k'_2{}^{i} + k'_1{}^{i+1}) c_{\mathrm{BL_i}} + k'_2{}^{i+1} c_{\mathrm{BL_{i+1}}}
\end{aligned}\right\} \qquad (1)$$

where ∇^2 is the Laplacian operator (given in Section SI1 of the Supporting Information for the main electrode geometries), $0 \le i \le n$ for the different complexes, $\mathrm{AL}_0 = \mathrm{A}$, $\mathrm{BL}_0 = \mathrm{B}$, $k_j{}^{0} = k_j{}^{n+1} = k'_j{}^{0} = k'_j{}^{n+1} = 0$ ($j = 1, 2$) and other symbols are defined in the Appendix.

The boundary value problem associated to the reduction of species A is given by

$$\begin{array}{l} t = 0, \quad q \ge q_s \\ t \ge 0, \quad q \to \infty \end{array} \left\{ \begin{array}{l} c_{\mathrm{A}}(q,0) = c_{\mathrm{A}}(\infty,t) = \dfrac{c^*}{1+\sum_{s=1}^{n}\beta_{\mathrm{s}}} \quad ; \quad c_{\mathrm{AL_i}}(q,0) = c_{\mathrm{AL_i}}(\infty,t) = \dfrac{c^*\beta_i}{1+\sum_{s=1}^{n}\beta_{\mathrm{s}}} \\ c_{\mathrm{B}}(q,0) = c_{\mathrm{B}}(\infty,t) = 0 \quad ; \quad c_{\mathrm{BL_i}}(q,0) = c_{\mathrm{BL_i}}(\infty,t) = 0 \end{array} \right. \qquad (2)$$

$t>0$, $q = q_s$:

$$\left.\begin{aligned} D_{\mathrm{A}}\left(\frac{\partial c_{\mathrm{A}}}{\partial q_{\mathrm{N}}}\right)_{q=q_s} &= -D_{\mathrm{B}}\left(\frac{\partial c_{\mathrm{B}}}{\partial q_{\mathrm{N}}}\right)_{q=q_s} \\ D_{\mathrm{AL_i}}\left(\frac{\partial c_{\mathrm{AL}_i}}{\partial q_{\mathrm{N}}}\right)_{q=q_s} &= -D_{\mathrm{BL_i}}\left(\frac{\partial c_{\mathrm{BL}_i}}{\partial q_{\mathrm{N}}}\right)_{q=q_s} \end{aligned}\right\} 1 \le i \le n \tag{3}$$

$$\left.\begin{aligned} c_{\mathrm{A}}\,(q_{\mathrm{s}}) &= c_{\mathrm{B}}(q_{\mathrm{s}})\, e^{\eta_{\mathrm{A/B}}} \\ c_{\mathrm{AL_i}}(q_{\mathrm{s}}) &= c_{\mathrm{BL_i}}(q_{\mathrm{s}})\, e^{\eta_{\mathrm{AL_i/BL_i}}} \end{aligned}\right\} 1 \le i \le n \tag{4}$$

with

$$\left.\begin{aligned} \eta_{\mathrm{A/B}} &= F\left(E - E^{\ominus'}_{\mathrm{A/B}}\right)/RT \\ \eta_{\mathrm{AL_i/BL_i}} &= F\left(E - E^{\ominus'}_{\mathrm{AL_i/BL_i}}\right)/RT \end{aligned}\right\} 1 \le i \le n \tag{5}$$

where q and t refer to the spatial-coordinate and time values, respectively, q_{s} to the coordinates at the electrode surface, q_{N} is the normal coordinate value at the surface of the electrode, β_i represents the overall formation constant for the different complexes of species A that are initially present in solution (see Eqs.(6)), and other symbols are defined in the Appendix.

We assume that the rates of formation and dissociation of the different complexes (k_1^i, $k_1'^i$, k_2^i and $k_2'^i$) are sufficiently fast in comparison to the diffusion rate such that complex formation and dissociation are at equilibrium even when current is flowing [9], i.e., that chemical equilibrium conditions are maintained at any point of the solution and time of the experiment,

$$\left.\begin{aligned} K_{\mathrm{m}} &= \frac{c_{\mathrm{AL_m}}(q,t)}{c_{\mathrm{AL_{m-1}}}(q,t)\,c_{\mathrm{L}}^{*}}, \quad K'_{\mathrm{m}} = \frac{c_{\mathrm{BL_m}}(q,t)}{c_{\mathrm{BL_{m-1}}}(q,t)\,c_{\mathrm{L}}^{*}} \\ \beta_i &= \prod_{m=1}^{i} K_{\mathrm{m}} c_L^{*} = \frac{c_{\mathrm{AL_i}}(q,t)}{c_{\mathrm{A}}(q,t)}, \quad \beta'_i = \prod_{m=1}^{i} K'_{\mathrm{m}} c_L^{*} = \frac{c_{\mathrm{BL_i}}(q,t)}{c_{\mathrm{B}}(q,t)} \end{aligned}\right\} \quad \forall\, q,t \;\; ; \;\; i \ge 1 \tag{6}$$

with the different symbols being defined in the Appendix.

To solve the problem defined above, the new variables $c_{\mathrm{T}}^{\mathrm{A}}$ and $c_{\mathrm{T}}^{\mathrm{B}}$, are defined [10] as

$$c_{\mathrm{T}}^{\mathrm{A}}(q,t) = c_{\mathrm{A}}(q,t) + \sum_{i=1}^{n} c_{\mathrm{AL}_i}(q,t) \tag{7}$$

$$c_{\mathrm{T}}^{\mathrm{B}}(q,t) = c_{\mathrm{B}}(q,t) + \sum_{i=1}^{n} c_{\mathrm{BL}_i}(q,t) \tag{8}$$

which relate to the total concentration of species A and B. Taking into account Eqs. (6)-(8), the diffusive-kinetic differential equation system and the boundary value problem simplify to:

$$\left.\begin{aligned} \frac{\partial c_{\mathrm{T}}^{\mathrm{A}}}{\partial t} &= D_{\mathrm{eff}}^{\mathrm{A}} \nabla^2 c_{\mathrm{T}}^{\mathrm{A}} \\ \frac{\partial c_{\mathrm{T}}^{\mathrm{B}}}{\partial t} &= D_{\mathrm{eff}}^{\mathrm{B}} \nabla^2 c_{\mathrm{T}}^{\mathrm{B}} \end{aligned}\right\} \tag{9}$$

$$\left.\begin{aligned} t = 0, \quad q \geq q_{\mathrm{s}} \\ t \geq 0, \quad q \to \infty \end{aligned}\right\} \qquad c_{\mathrm{T}}^{\mathrm{A}}(q,0) = c_{\mathrm{T}}^{\mathrm{A}}(\infty,t) = c^{*} \quad ; \quad c_{\mathrm{T}}^{\mathrm{B}}(q,0) = c_{\mathrm{T}}^{\mathrm{B}}(\infty,t) = 0 \tag{10}$$

$$t > 0,\ q = q_{\mathrm{s}} \left\{ \begin{aligned} & D_{\mathrm{eff}}^{\mathrm{A}} \left(\frac{\partial c_{\mathrm{T}}^{\mathrm{A}}}{\partial q} \right)_{q=q_s} = -D_{\mathrm{eff}}^{\mathrm{B}} \left(\frac{\partial c_{\mathrm{T}}^{\mathrm{B}}}{\partial q} \right)_{q=q_s} \\ & c_{\mathrm{T}}^{\mathrm{A}}(q_s) = c_{\mathrm{T}}^{B}(q_s)\, \omega\, \mathrm{e}^{\eta_{\mathrm{A/B}}} \end{aligned} \right. \tag{11}$$

where $c_{\mathrm{T}}^{\mathrm{A}}(q_{\mathrm{s}})$ and $c_{\mathrm{T}}^{\mathrm{B}}(q_{\mathrm{s}})$ are the total surface concentrations of species A and B (see Eqs.(7) and (8), respectively) and

$$\omega = \frac{1 + \sum_{i=1}^{n} \beta_i}{1 + \sum_{i=1}^{n} \beta_i'} \ , \quad D_{\mathrm{eff}}^{\mathrm{A}} = \frac{D_{\mathrm{A}} + \sum_{i=1}^{n} D_{\mathrm{AL}_i} \beta_i}{1 + \sum_{i=1}^{n} \beta_i} \ , \quad D_{\mathrm{eff}}^{\mathrm{B}} = \frac{D_{\mathrm{B}} + \sum_{i=1}^{n} D_{\mathrm{BL}_i} \beta_i'}{1 + \sum_{i=1}^{n} \beta_i'} \tag{12}$$

with $D_{\mathrm{eff}}^{\mathrm{A}}$ and $D_{\mathrm{eff}}^{\mathrm{B}}$ being the effective diffusion coefficients of the pseudo-species $\mathrm{A_T}$ and $\mathrm{B_T}$, respectively. In the situation where the concentrations of all the species satisfy chemical equilibrium conditions (Eqs.(6)), $D_{\mathrm{eff}}^{\mathrm{A/B}}$ is simply equal to a mole fraction weighted average [11]. By assuming that $D_{\mathrm{eff}}^{\mathrm{A}} = D_{\mathrm{eff}}^{\mathrm{B}} = D$, which does not mean that the diffusivities of the free and complexed species are the same and it is reasonable for a

great variety of experimental systems in conventional solvents, the expression for the current for any value of the applied potential in the different geometries considered can be written in the following general form (as demonstrated in Section SI2 in the Supporting Information):

$$\frac{I(q,t)}{FA_{\mathrm{G}}D} = (c^{*} - c_{\mathrm{T}}^{\mathrm{A}}(q_{\mathrm{s}}))\,\mathrm{f}_{\mathrm{G}}(q_{\mathrm{G}},\mathrm{t}) \;=\; c_{\mathrm{T}}^{\mathrm{B}}(q_{\mathrm{s}})\,\mathrm{f}_{\mathrm{G}}(q_{\mathrm{G}},\mathrm{t}) \tag{13}$$

where $\mathrm{f}_{\mathrm{G}}(q_{\mathrm{G}},\mathrm{t})$ is a function of time and the electrode geometry, given in Table 1 for the most commonly-used electrodes, and A_{G} is the electrode area.

2.2 *Application of an arbitrary sequence of consecutive pulses*

Next we consider the application of any succession of potential steps E_1, E_2, ... E_{p} of duration τ. The general solution corresponding to the *p*-th applied potential can be easily obtained on account of the fact that we have a linear problem and, therefore, any linear combination of solutions is also a solution of the problem, and also that the interfacial concentrations of all the participating species only depend on the applied potential; that is, they are independent of the previous "history" of the experiment regardless of the electrode geometry considered (see Section SI2 in Supporting Information). The two above conditions imply that the superposition principle can be applied [12] in such a way that the solution for the current corresponding to the application of the *p*-th potential can be written as follows:

$$\frac{I_{\mathrm{p}}}{FA_{\mathrm{G}}D} = \sum_{m=1}^{\mathrm{p}} \left(c_{\mathrm{T}}^{\mathrm{A(m-1)}} - c_{\mathrm{T}}^{\mathrm{A(m)}}\right) \mathrm{f}_{\mathrm{G}}\left(q_{\mathrm{G}},(p-m+1)\tau\right) \tag{14}$$

where

$$c_{\mathrm{T}}^{\mathrm{A(m-1)}} - c_{\mathrm{T}}^{\mathrm{A(m)}} = c^{*} Z_{\mathrm{m}} = c^{*}\left(\frac{1}{1+\omega J_{\mathrm{m}}} - \frac{1}{1+\omega J_{\mathrm{m-1}}}\right) \tag{15}$$

and J_{m} is given by

$$J_{\mathrm{m}} = \exp\left\{\frac{F}{RT}(E_{\mathrm{m}} - \mathrm{E}^{\ominus'}_{\mathrm{A/B}})\right\}, \quad m \geq 1\Big\} \tag{16}$$

and $\mathrm{f_G}\left(q_G, t\right)$ is defined in Table 1 for each electrode geometry. As for Eq. (13), Eq. (14) is formally identical to that corresponding to a simple reversible electron transfer process [13, 14], the dependence on the different complexation reactions being contained in the parameter ω (Eqs. (12)).

Eq. (14) can be applied to any sequence of *N* constant potential pulses and so to any voltammetric technique. In this work, we will focus on the two most popular voltammetric techniques (see SI2 in Supporting Information): cyclic voltammetry,

$$\Psi_{\mathrm{CV}} = \sqrt{\frac{D}{a}} \sum_{m=1}^{\mathrm{p}} \pm \frac{\omega J_{\mathrm{m}} \Delta\eta}{\left(1 + \omega J_{\mathrm{m}}\right)^2} \cdot \mathrm{f_G}\left(q_{\mathrm{G}}, (p - m + 1)\tau\right); \;\; p = 1, 2\ldots, N \tag{17}$$

with *N* being the total number of pulses applied and:

$$a = \frac{Fv}{RT} \tag{18}$$

$$\Psi_{\mathrm{CV}} = \frac{I_{\mathrm{p}}}{FA_{\mathrm{G}}c^*\sqrt{Da}} \tag{19}$$

$$\Delta\eta = \frac{F}{RT}\Delta E \tag{20}$$

and square wave voltammetry,

$$\psi_{\mathrm{SW}} = \frac{I_{\mathrm{SW}}}{FA_{\mathrm{G}}Dc^*} = \left\{\sum_{m=1}^{2\mathrm{p}-1} Z_{\mathrm{m}} \cdot \mathrm{f_G}\left(q_G, (p - m + 1)\tau\right) - \sum_{m=1}^{2\mathrm{p}} Z_{\mathrm{m}} \cdot \mathrm{f_G}\left(q_{\mathrm{G}}, (p - m + 1)\tau\right)\right\} \tag{21}$$

with:

$$I_{\mathrm{SW}} = I_{2\mathrm{p}-1} - I_{2\mathrm{p}} = I_f - I_b \; ; \quad p = 1, 2\ldots, N/2 \tag{22}$$

and $\mathrm{f_G}$ and A_{G} being given in Table 1. Expressions for the CV and SWV responses under stationary conditions are gathered in Section SI2 of the Supporting Information.

3. EXPERIMENTAL

3.1 *Chemical reagents*

Anthraquinone ($C_{14}H_8O_2$, Fluka, ≤99%), ferrocene ($Fe(C_5H_5)_2$, Aldrich, 98%), acetonitrile (MeCN, Sigma-Aldrich, 99.8%) tetrabutylammonium hexafluorophosphate ($TBAPF_6$, Fluka, ≥99%), ferrocenium hexafluorophosphate ($FcPF_6$, Sigma Aldrich, 97%), hexaammineruthenium (III) chloride (Ruhex(III), Aldrich, 98%) and potassium nitrate (KNO_3, Merck, ISO Reag.) were all used as received without further purification

3.2 *Instrumentation*

All electrochemical measurements were performed with a homebuilt potentiostat. A Pt wire was used as counter electrode, a silver wire as pseudo-reference electrode and a gold microdisk of radius 12.4 μm (encompassed within a 3 mm-diameter insulating sheath) was employed as working electrode.

The UV-Vis spectra were recorded with a spectrophotometer p*-180 of “Applied Photophysics” and the conductivity measurements were performed with an EC-Meter GLP 31 CRISON with built-in temperature correction.

4. RESULTS AND DISCUSSION

4.1 *Theoretical results*

From the analytical equations obtained for CV and SWV (Eqs. (17) and (21)) the study of the current-potential response in these techniques will be performed as well as the analysis of the influence of the key system variables. First, the effect of the parameter ω (Eqs. (12)) is shown in Fig. 1 for a spherical electrode of 50 μm-radius. Note that large ω-values relate to the situation where the complexes of the reactant species A are more stable than those of species B, whereas the opposite situation is found for small ω-values. As can be observed, the only influence of this parameter is the shift of the curves towards more negative potentials when ω increases on account of the hindering of the electro-reduction reaction due to the stabilitization of the oxidized species with respect to the reduced ones. According to Eqs. (9)-(11), the peak potential in SWV coincides with the half wave potential [15] ($E_{\text{peak}} = E_{1/2}$) such that:

$$E_{\text{peak}} = E^{\ominus'}_{\text{A/B}} + \frac{RT}{F}\ln\left(\frac{1}{\omega}\right) \tag{23}$$

In practice, the influence of the ω-value on the voltammograms can be revealed experimentally by changing the bulk concentration of species L (c^*_{L}), that is, of the complexing agent, protons, counterions,… In this respect, Fig. 2 shows the variation of the peak potential in SWV (E_{peak}) with c^*_{L} for the $C^{eq}E^{rev}C^{eq}$ mechanism (i.e., a coupled chemical reaction takes place "before" and "after" the electron transfer). As can be observed, the variation of the signal position informs about the relative stability of the oxidized and reduced species. When $K/K' > 1$, the stabilization of the oxidized species by the chemical equilibrium is greater and the voltammograms move towards more negative overpotentials, whereas the opposite is true for $K/K' < 1$. Note that these

situations include as limit cases the $C^{eq}E^{rev}$ and $E^{rev}C^{eq}$ mechanisms, where $K' = 0$ and $K = 0$, respectively.

As shown in Fig. 2, in the absence of coupled reactions (the so-called E mechanism) the voltammetry is insensitive to changes in the concentration of species L provided that this does not lead to significant changes in the ionic strength. Therefore, the study of the position of the voltammograms in presence of different concentrations of species L offers a simple criterion to discriminate between simple electron transfer processes and those complicated by coupled chemical equilibria.

The effect of the electrode geometry and size is shown in Fig. 3, where SWV and CV curves are plotted for ω=5 and different values of the characteristic dimensions of microelectrodes of different geommetries (r_s, r_d and $w/2$ for spheres, disks and bands respectively with $r_s = r_d = w/2$). For large electrodes (Fig. 3a) the curves (i.e., the current density) show little difference because diffusion is almost planar and the electrode geometry plays a less important role. These differences are enhanced as the electrode size is decreased. Regardless of the electrode size, the SWV voltammograms show a peak shape so that the determination of the signal position at microelectrodes is easier and more accurate than in CV. Moreover, the position of the voltammograms is not influenced by the electrode geometry and size so that small uncertainties in their determination do not affect the quantitative study of the chemical equilibria. Thus, the experimental study in this work will be performed by using SWV in combination with microelectrodes where capacitative and ohmic drop effects are greatly reduced. In particular a gold microdisk will be used attending to the ubiquity of this electrode geometry in electrochemical measurements due to the easier fabrication and surface cleaning with respect to other shapes.

4.2 *Experimental study of the ion pairing between* $AQ^{\bullet-}$ *and* NBu_4^+

Radical species are highly reactive so that their study is challenging, electrochemical methods being valuable given that unstable species can be electrogenerated and immediately studied in the working solution. In this paper, the species under study is the radical anion ($AQ^{\bullet-}$) formed in the reversible one-electron reduction of anthraquinone in deoxygenated acetonitrile and in presence of $TBAPF_6$ as supporting electrolyte. The $AQ^{\bullet-}$ species may form an ion pair with the tetrabutylammonium cation (NBu_4^+) of the supporting electrolyte according to the following $E^{rev}C^{eq}$ mechanism:

$$\left.\begin{array}{l} AQ + e^- \rightleftarrows AQ^{\bullet-} \\ AQ^{\bullet-} + NBu_4^+ \rightleftarrows \left[NBu_4^+ AQ^{\bullet-}\right] \end{array}\right\} \qquad \text{Scheme II}$$

and, as discussed above, the association equilibrium constant can be determined *via* square wave voltammetry.

4.2.1 *Ion pairing between the supporting electrolyte ions*

The supporting electrolyte ($TBAPF_6$) may be partially associated as ion pairs

$$NBu_4^+ + PF_6^- \rightleftarrows \left[NBu_4^+ PF_6^-\right] \qquad \text{Scheme III}$$

such that all the tetrabutylammonium of the medium is not available to associate with the electrogenerated species. This reaction has been quantified in the present work by conductivity measurements in $TBAPF_6$ acetonitrile solutions based on the decrease in the solution conductivity upon the formation of electroneutral ion pairs [16].

The Fuoss-Hsia equation modified by Fernández-Prini for 1:1 electrolytes [17-19] was employed for the quantitative analysis:

$$\Lambda = \Lambda_0 - S\sqrt{c\theta} + E\,c\theta\ln(c\theta) + J_1\,c\theta - J_2\,(c\theta)^{3/2} - K_a c\theta\, f_\pm^2\,\Lambda \qquad (24)$$

with θ being the degree of dissociation, $f_{\pm}$ the mean ionic activity coefficient and K_a the equilibrium constant of association based on activities:

$$K_a = \frac{(1-\theta)}{\frac{c}{c^0}\theta^2 f_{\pm}^2} \tag{25}$$

where it has been considered that the activity coefficient of the ion pair is the unity and c^0 = 1 M. The coefficient $f_{\pm}$ has been calculated from the extended form of the Debye-Hückel equation [20], using the Bjerrum distance [21] as the distance of closest approach between ions. The remaining terms of Eq. (24) are defined in the Supporting Information (Section SI4).

By fitting of the experimental molar conductivity for different electrolyte concentrations, the association constant and the limit molar conductivity (Λ_0) have been determined. The quality of the fitting has been evaluated from the value of the sum of squared differences (SSD)

$$\mathrm{SSD} = \sum_{i=1}^{N} (y_{\mathrm{exp}} - y_{\mathrm{sim}})_i^2 \tag{26}$$

where y_{exp} and y_{sim} are the N experimental and simulated data points. The optimum values found from a set of three independent measurements were $K_a(\mathrm{NBu_4PF_6})$ = 78±3 and $\Lambda_0(\mathrm{NBu_4PF_6})$ = 166±7 S cm^2 mol^{-1}. The $K_a(\mathrm{NBu_4PF_6})$ value obtained is consistent with the data reported in the literature in acetonitrile [22] as well as those in other solvents of similar dielectric constant [23].

4.2.2 *Square wave voltammetry study*

The association between $\mathrm{AQ}^{\bullet-}$ and $\mathrm{NBu_4^+}$ has been studied by square wave voltammetry at different concentrations of supporting electrolyte, this always being

sufficiently greater than that of anthraquinone ($c^*_{\mathrm{TBAPF_6}} \geq 60 c^*_{\mathrm{AQ}}$) such that the kinetics of the ion pairing can be considered of (pseudo)first order and the ohmic drop is minimized [24].

The presence of water in the electrolyte solution is undesirable because of the rapid protonation of the radical species that leads to the two-electron reduction of anthraquinone [25, 26]:

$$\mathrm{AQ} + 2\mathrm{H}^+ + 2e^- \rightleftarrows \mathrm{AQH_2} \qquad \text{Scheme IV}$$

Thus, in order to minimize water contamination as well as uncertainties related to junction potentials [27], a silver wire was employed as pseudo-reference electrode [28, 29]. For accurate comparison of the potential data, the redox couple ferrocene/ferrocenium was used as an internal reference [30-33]. Ion association between the ferrocenium cation and the supporting electrolyte anion ($\mathrm{PF_6^-}$) was discarded by UV-Vis absorption measurements (Section SI5 of the Supporting Information) such that the redox couple $\mathrm{Fc/Fc^+}$ is suitable as an internal reference in this medium. Thus, SWV experiments for the reduction of anthraquinone and for the oxidation of ferrocene were recorded, and the peak potential values for anthraquinone are referred to the ferrocene peak.

In the theoretical modeling of the problem, ideal solutions were considered and activity coefficients were set equal to unity. However, experiments were performed in real solutions and the corresponding ionic strength correction must be introduced. Thus, the association thermodynamic constant based on activities is defined by

$$K'^{\mathrm{AQ}}_{\mathrm{a}} = \frac{a_{\mathrm{NBu_4AQ}}}{a_{\mathrm{NBu_4^+}} a_{\mathrm{AQ^-}}} = \frac{c_{\mathrm{NBu_4AQ}} f_{\mathrm{NBu_4AQ}}}{\left(c_{\mathrm{NBu_4^+}} f_{\mathrm{NBu_4^+}}\right)\left(c_{\mathrm{AQ^-}} f_{\mathrm{AQ^-}}\right)} = \frac{K'^{\mathrm{AQ}}}{f_\pm^2} \tag{27}$$

with $f_\pm$ being the mean ionic activity coefficient (it has been considered that the activity coefficient for the ion pair is the unity) and K'^{AQ} the equilibrium constant based on concentrations.

For the ion association in Scheme II, the ω parameter (see Eqs. (6), (12) and (27)) is given by:

$$\omega_{AQ} = \frac{1}{1 + K'^{AQ} c^*_{TBAPF_6}} = \frac{1}{1 + K'^{AQ}_a f_\pm^2 c^*_{TBAPF_6}} \tag{28}$$

whereas for ferrocene

$$\omega_{Fc} = 1 \tag{29}$$

with $c^*_{TBAPF_6}$ being the *free* concentration of tetrabutylammonium. From Eq.(23), one obtains that

$$E^{Fc}_{peak} = E^{\ominus'}_{Fc^+/Fc} \tag{30}$$

$$E^{AQ}_{peak} = E^{\ominus'}_{AQ/AQ^{\bullet-}} + \frac{RT}{F} \ln\left[1 + K'^{AQ}_a f_\pm^2 c^*_{TBAPF_6}\right] \tag{31}$$

with

$$E^{\ominus'}_{Fc^+/Fc} = E^0_{Fc^+/Fc} + \frac{RT}{F} \ln\left(f_{Fc^+}\right) \tag{32}$$

$$E^{\ominus'}_{AQ/AQ^{\bullet-}} = E^0_{AQ/AQ^{\bullet-}} + \frac{RT}{F} \ln\left(\frac{1}{f_{AQ^-}}\right) \tag{33}$$

where it has been assumed that the activity coefficients of neutral species are the unity.

The peak potentials for the reduction of anthraquinone (Scheme II) are referred to the peak potentials of ferrocene, as shown in Fig.4, by using Eqs. (30) and (31)

$$E^{AQ}_{peak} - E^{Fc}_{peak} = \left(E^0_{AQ/AQ^{\bullet-}} - E^0_{Fc^+/Fc}\right) + \frac{RT}{F} \ln\left[\frac{1}{f_\pm^2}\right] + \frac{RT}{F} \ln\left[1 + K'^{AQ}_a f_\pm^2 c^*_{TBAPF_6}\right] \tag{34}$$

with

$$f_\pm^2 = \left(f_{NBu_4^+} f_{AQ^-}\right) = \left(f_{Fc^+} f_{AQ^-}\right) \tag{35}$$

Eq. (34) has been used to fit the experimental values with $E^0_{AQ/AQ^{\bullet-}} - E^0_{Fc^+/Fc}$ and K'^{AQ}_a as adjustable parameters. The values that minimize the sum of squared differences (SSD) are $E^0_{AQ/AQ^{\bullet-}} - E^0_{Fc^+/Fc} = -1.318 \pm 0.002$ V and $K'^{AQ}_a = 300 \pm 50$, with the ± values

corresponding to the asymptotic standard errors. As can be observed in Figure 4a, the above $E^0_{AQ/AQ^{\bullet-}} - E^0_{Fc^+/Fc}$ and K'^{AQ}_a values lead to satisfactory fittings of the position and shape of all the experimental SWV curves. This also indicates that possible ohmic drop distortions are negligible. Thus, the SWV peaks are smaller and broader in the presence of significant ohmic drop, that is, smaller peak currents and larger half-peak widths ($w_{1/2}$) are observed [34]. For a fully-reversible electrode reaction, the $w_{1/2}$ value is determined by the square wave amplitude (E_{SW}), being independent of the electrode geometry and frequency employed [35]:

$$w_{1/2} = \frac{RT}{F} \ln \left[\frac{1 + e^{2\eta_{SW}} + 4e^{\eta_{SW}} + \sqrt{\left(1 + e^{2\eta_{SW}} + 4e^{\eta_{SW}}\right)^2 - 4e^{2\eta_{SW}}}}{1 + e^{2\eta_{SW}} + 4e^{\eta_{SW}} - \sqrt{\left(1 + e^{2\eta_{SW}} + 4e^{\eta_{SW}}\right)^2 - 4e^{2\eta_{SW}}}} \right] \qquad (36)$$

where $\eta_{SW} = \frac{F}{RT} E_{SW}$. The experimental $w_{1/2}$ value in the present study is 100 ± 5 mV, which compares well with the value predicted by Eq. (36), $w_{1/2} = 103$ mV, for the E_{SW} value of the SWV experiments ($E_{SW} = 30$ mV). This result confirms both the reversible nature of the electrode process and the absence of ohmic drop effects in spite of the small concentrations of supporting electrolyte in some of the measurements, which illustrate the benefits of the use of microelectrodes. Note that the theory presented here as well as the experimental approach are general and suitable for the study of other chemical processes of interest in different contexts such as complexations[9, 36], protonation-deprotonations [37-40] or isomerizations[41, 42].

5. CONCLUSIONS

A simple explicit solution has been derived to assist the use of electrochemical techniques in speciation studies. The solution is valid for electrode processes where none, one or both electroactive species are involved in chemical equilibria in solution, and it is applicable to any voltammetric technique whatever the size and shape of the working electrode employed.

The theoretical results demonstrate that the use of square wave voltammetry at microelectrodes is very adequate for the identification and characterization of the reaction mechanism from the variation of the position of the voltammograms. Thus, the advantages of microelectrodes hold (mainly low ohmic drop and capacitative distorting effects) whereas well-defined peak-shaped signals are obtained that can be analyzed more accurately than sigmoid voltammograms recorded in cyclic voltammetry. Also, the position of the peak is independent of the microelectrode size and shape, which is highly beneficial given that errors associated to uncertainties of the electrode geometry are avoided. Accordingly, a simple analytical expression has been derived for the peak potential in SWV, which enables straightforward and accurate determination of the standard potentials and equilibrium constants from SWV experiments at different concentrations of ligand.

Electrochemical methods are of particular interest in the study of unstable species given that the target species is generated and examined *in situ* and in a short period of time. In this respect, the theory has been applied to the study of the ion pairing between the anion radical of anthraquinone ($AQ^{\bullet -}$) and the tetrabutylaamonium cation (NBu_4^+) in acetonitrile medium, finding the values for the association constant and the standard potential of 300 ± 50 and -1.318 ± 0.002 V and (*vs* Fc/Fc^+), respectively.

ACKNOWLEDGMENTS

The authors greatly appreciate the financial support provided by the Ministerio de Economia y Competitividad (Project Number CTQ2012-36700, co-funded by European Regional Development Fund) and by the Fundacion Séneca de la Región de Murcia under the III PCTRM 2011-2014 Programme (Project 18968/JLI/13). EL also thanks the funding received from the European Union Seventh Framework Programme-Marie Curie COFUND (FP7/2007-2013) under UMU Incoming Mobility Programme ACTion (U-IMPACT) Grant Agreement 267143.

Appendix. Notation

Roman symbols

c^* total initial concentration of species A in solution ($c^* = c_A^* + \sum_{i=1}^{n} c_{AL_i}^*$)

c^0 standard concentration (1 M)

c_j^* initial concentration of species j (j = L, A, B, AL_i and BL_i ; $1 \le i \le n$)

$c_{TBAPF_6}^*$ free concentration of tetrabutylammonium

D_j diffusion coefficient of species j (j = A, B, AL_i and BL_i ; $1 \le i \le n$)

$E_{1/2}$ half wave potential

E_i^0 standard potential of the redox couple i

$E_{A/B}^{\ominus\prime}$ formal potential of the redox couple i

E_{peak} peak potential in SWV

F Faraday constant

f activity coefficient

$f_{\pm}$ mean ionic activity coefficient

k_j^i (j = 1, 2) forward and backward rate constants of the different complexation reactions of species A, taken to be pseudo-first order due to the high ligand concentration.

$k_j'^i$ (j = 1, 2) forward and backward rate constants of the different complexation reactions of species B, taken to be pseudo-first order due to the high ligand concentration.

K_i equilibrium constant based on concentrations for each complexation reaction of species A ($1 \le i \le n$).

K_i' equilibrium constant based on concentrations for each complexation reaction of species B ($1 \le i \le n$).

K_a, K_a' equilibrium constants based on activities

R molar gas constant

r_s sphere radius

r_d disk radius

T absolute temperature

w band width

$w_{1/2}$ half-peak width of the square wave voltammogram

Greek symbols

∇^2 Laplacian operator

β_i overall formation constant for the different complexes of species A ($1 \le i \le n$)

β_i' overall formation constant for the different complexes of species B ($1 \le i \le n$)

θ degree of dissociation

Λ molar conductivity

Λ_0 molar conductivity at infinite dilution

ω $\omega = \left(1 + \sum_{i=1}^{n} \beta_i\right) / \left(1 + \sum_{i=1}^{n} \beta_i'\right)$

Table 1. Expressions for the function $f_{\mathrm{G}}\left(q_G,t\right)$ and the area A_{G} of the main electrode geometries. $q_{\mathrm{G}} = r_{\mathrm{d}}$ for discs; $q_{\mathrm{G}} = r_{\mathrm{s}}$ for spheres or hemispheres; $q_{\mathrm{G}} = r_{\mathrm{c}}$ for cylinders; $q_{\mathrm{G}} = w$ for bands.

Electrode	**Function** $f_{\mathrm{G}}\left(q_G,t\right)$
Planar	$\frac{1}{\sqrt{\pi Dt}}$
Spherical (radius r_{s}, Area $A_{\mathrm{s}} = 4\pi r_{\mathrm{s}}^2$)	$\frac{1}{\sqrt{\pi Dt}} + \frac{1}{r_{\mathrm{s}}}$
Disc (radius r_{d}, $A_{\mathrm{d}} = \pi r_{\mathrm{d}}^2$)	$\frac{4}{\pi r_{\mathrm{d}}}\left(0.7854 + 0.44315\frac{r_{\mathrm{d}}}{\sqrt{Dt}} + 0.2146\exp\left(-0.39115\frac{r_{\mathrm{d}}}{\sqrt{Dt}}\right)\right)$
Cylindrical (radius r_{c}, length l, $\mathrm{A}_c = 2\pi r_{\mathrm{c}} l$)	$\frac{e^{-0.1(\pi Dt)^{1/2}/r_c}}{\sqrt{\pi Dt}} + \frac{1}{r_c}\frac{1}{\ln\left(5.2945 + 1.4986\frac{\sqrt{Dt}}{r_c}\right)}$
Band (height w, length l, $\mathrm{A_w} = wl$)	$\frac{1}{w} + \frac{1}{\sqrt{\pi Dt}}$ for $Dt / w^2 < 0.4$ $0.25\sqrt{\frac{\pi}{Dt}}e^{-0.4(\pi Dt)^{1/2}/w} + \frac{1}{w}\frac{\pi}{\ln\left(5.2945 + 5.9944\frac{\sqrt{Dt}}{w}\right)}$ for $Dt / w^2 \geq 0.4$

Figure 1. Influence of the parameter ω on the response in SWV (Eq. (21)) and CV (Eq. (17)) for a spherical electrode of radii 50 μm. SWV parameters: E_{SW}=30 mV, E_s=3mV, τ=10ms (f=50Hz). CV parameters: ΔE=0.01mV, v=100mV/s. T=298K, D=10^{-5} cm^2/s.

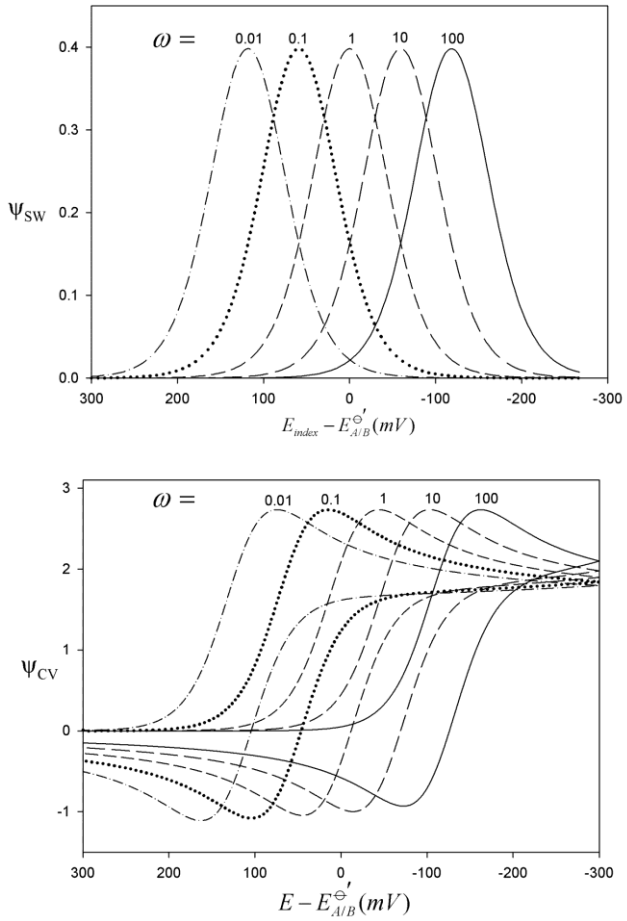

Figure 2. Variation of the SWV peak potential (Eq. (23)) with the concentration of the ligand $\left(c_{\mathrm{L}}^{*}\right)$ for a $C^{eq}E^{rev}C^{eq}$ mechanism with different K/K' values (given in the graph). It is assumed that the change of c_{L}^{*} does not lead to a significant variation of the ionic strength.

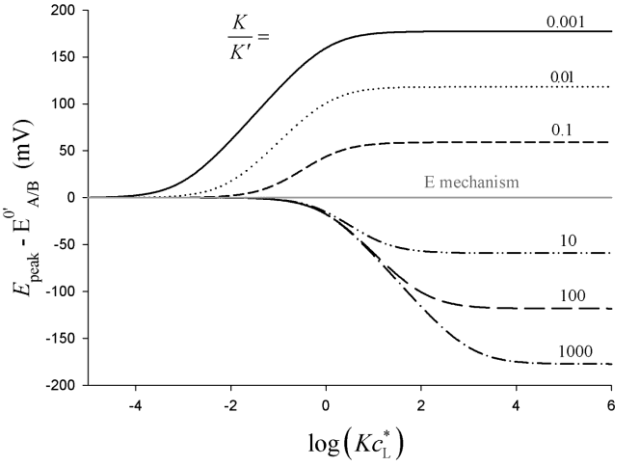

Figure 3. SWV (Eq. (21)) and CV (Eq. (17)) curves for electrodes of different geometries and characteristic dimensions (q_G=r_s=r_d=(w/2)) and ω=5. SWV parameters: E_{SW} = 30 mV, E_s = 3mV, τ = 10 ms (f = 50Hz). CV parameters: ΔE = 0.01mV, v=100mV/s. T=298K, D=$10^{-5}$$cm^2$/s.

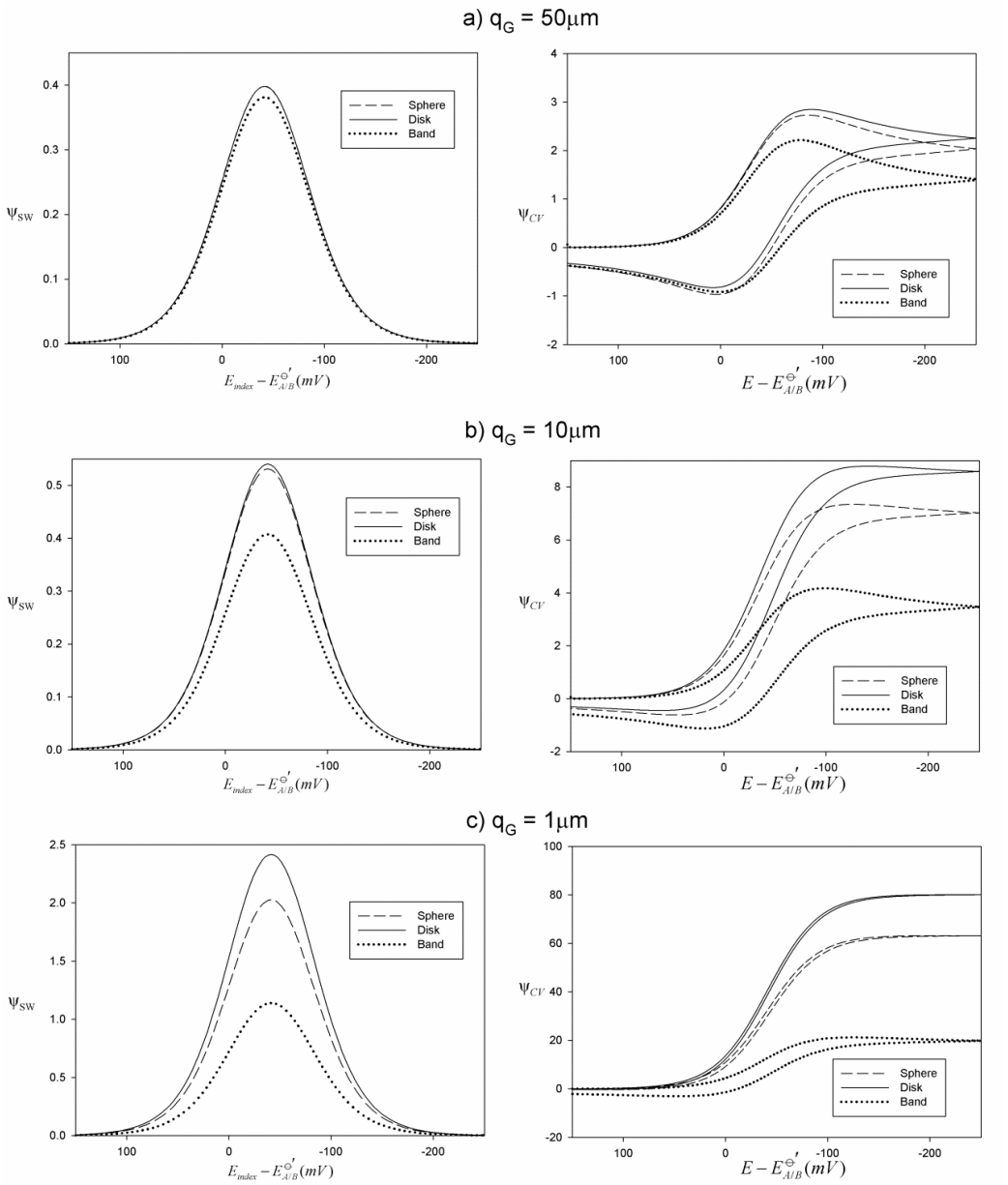

Figure 4. a) Experimental (points) and best-fit theoretical (solid line, Eq. (21)) voltammograms corresponding to the anthraquinone electro-reduction at different *free* concentrations of NBu_4^+ (calculated according to the association equilibrium constant determined in Section 4.2.1) at a gold microdisk of radii 12.4 μm. E_s=3mV, f=50Hz, E_{SW}=30mV, T=298K. **b)** Fitting of the experimental values of the peak potentials of the square wave voltammograms shown in Figure 4a according to Eq. (34). Error bars correspond to the standard deviation of three SWV experiments at each concentration of NBu_4^+.

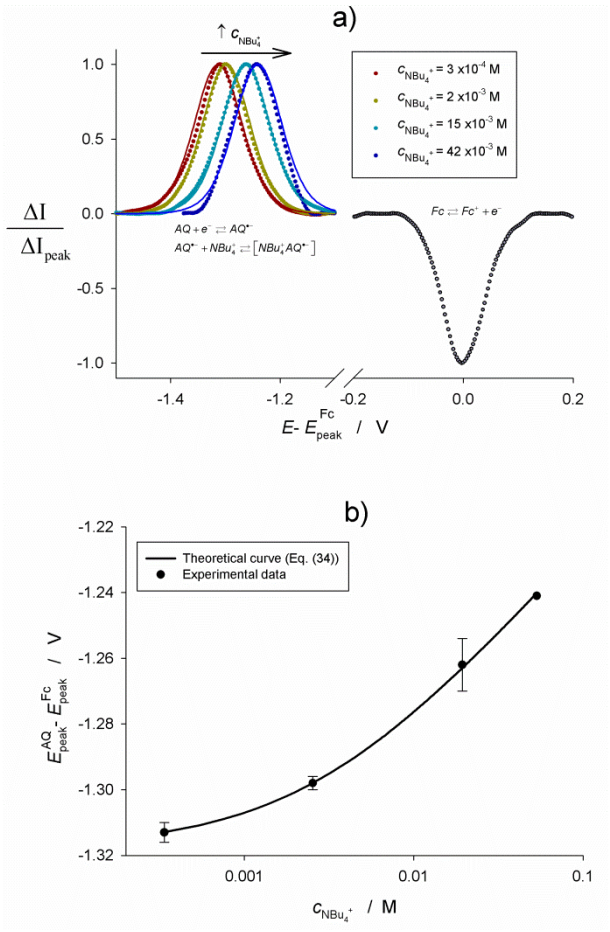

REFERENCES

(1) Bard, A. J.; Faulkner, L. R. *Electrochemical Methods. Fundamentals and Applications*; Wiley: New York, 2001; ch 12.
(2) Compton, R. G.; Banks, C. E. *Understanding Voltammetry*, Second ed.; Imperial College Press: London, 2011; ch 7.
(3) Campos-Martin, J. M.; Blanco-Brieva, G.; Fierro, J. L. G. *Angew. Chem. Int. Ed.* **2006**, *45*, 6962.
(4) Menna, P.; Salvatorelli, E.; Minotti, G. *Chem. Res. Toxicol.* **2010**, *23*, 6.
(5) Sirés, I.; Brillas, E. *Environment International* **2012**, *40*, 212.
(6) Jürmann, G.; Schiffrin, D. J.; Tammeveski, K. *Electrochim. Acta* **2007**, *53*, 390.
(7) Sarapuu, A.; Helstein, K.; Vaik, K.; Schiffrin, D. J.; Tammeveski, K. *Electrochim. Acta* **2010**, *55*, 6376.
(8) Seinberg, J.; Kullapere, M.; Maëorg, U.; Maschion, F. C.; Maia, G.; Schiffrin, D. J.; Tammeveski, K. *J. Electroanal.Chem* **2008**, *624*, 151.
(9) Molina, A.; Torralba, E.; Serna, C.; Ortuño, J. A. *Electrochim. Acta* **2013**, *106*, 244.
(10) Puy, J.; Mas, F.; Díaz-Cruz, J. M.; Esteban, M.; Cassasas, E. *Anal. Chim. Acta* **1992**, *268*, 261.
(11) Texter, J. *J. Electroanal. Chem* **1991**, *304*, 257.
(12) Molina, A.; Serna, C.; Camacho, L. *J. Electroanal. Chem* **1995**, *394*, 1.
(13) Molina, A.; González, J.; Henstridge, M.; Compton, R. G. *J. Phys. Chem. C* **2011**, *115*, 4054.
(14) Molina, A.; González, J.; Laborda, E.; Compton, R. G. *Russ. J. Electrochem.* **2012**, *48*, 600.
(15) Aoki, K.; Maeda, K.; Osteryoung, J. *J. Electroanal. Chem* **1989**, *272*, 17.
(16) Marcus, Y.; Hefter, G. *Chem. Rev* **2006**, *106*, 4585.
(17) Fernandez-Prini, R. *Trans. Faraday Soc.* **1969**, *65*, 3311.
(18) Miyoshi, K. *Bull. Chem. Soc. Jpn.* **1973**, *46*, 426.
(19) Yeager, H. L.; Kratochvil, B. *Can. J. Chem.* **1975**, *53*, 3448.
(20) Debye, P.; Hückel, E. *Physik. Z* **1923**, *24*, 185.
(21) Bjerrum, N. *K. Dan. Vidensk. Selsk.* **1926**, *7*, No.9.
(22) Tsierkezos, N. G.; Philippopoulos, A. I. *Fluid Phase Equilibria* **2009**, *277*, 20.
(23) Roy, M. N.; Ekka, D.; Dewan, R. *Fluid Phase Equilibria* **2012**, *314*, 113.
(24) Dickinson, E. J. F.; Limon-Petersen, J. G.; Rees, N. V.; Compton, R. G. *J. Phys. Chem. C* **2009**, *113*, 11157.
(25) Batchelor-McAuley, C.; Li, Q.; Dapin, S. M.; Compton, R. G. *J. Phys. Chem. B* **2010**, *114*, 4094.
(26) Guin, P. S.; Das, S.; Mandal, P. C. *Int. J. Electrochem. Sci.* **2011**, *816202*.
(27) Mousavi, M. P. S.; Bühlmann, P. *Analytical Chemistry* **2013**, *85*, 8895.
(28) Inzelt, G.; Lewenstam, A.; Scholz, F. *Handbook of Reference Electrodes*; Springer: Berlin, 2013.
(29) Izutsu, K. *Electrochemistry in nonaqueous solutions*; John Wiley & Sons, 2009.
(30) Barrière, F.; Geiger, W. E. *J. Am. Chem. Soc.* **2006**, *128*, 3980.
(31) Gritzner, G.; Kuta, J. *Pure Appl. Chem.* **1984**, *56*, 461.
(32) Lehmann, M. W.; Evans, D. H. *J. Phys. Chem. B* **1998**, *102*, 9928.
(33) Macías-Ruvalcaba, N. A.; Evans, D. H. *J. Phys. Chem. B* **2005**, *109*, 14642.
(34) Mirceski, V.; Lovric, M. *J. Electroanal. Chem.* **2001**, *497*, 114.
(35) Molina, A.; Gonzalez, J.; Laborda, E.; Compton, R. G. *Russ J Electrochem* **2012**, *48*, 600.

(36) Beer, P. D.; Gale, P. A.; Chen, G. Z. *Coord. Chem. Rev.* **1999**, *185*, 3.
(37) Alligrant, T. M.; Alvarez, J. C. *J. Phys. Chem. C* **2011**, *115*, 10797.
(38) Canaguier, S.; Fourmond, V.; Perotto, C. U.; Fize, J.; Pécaut, J.; Fontecave, M.; Field, M. J.; Artero, V. *Chem. Commun.* **2013**, *49*, 5004.
(39) Costentin, C.; Robert, M.; Savéant, J. M.; Tard, C. *Acc. Chem. Res.* **2014**, *47*, 271.
(40) Weinberg, D. R.; Gagliardi, C. J.; Hull, J. F.; Murphy, C. F.; Kent, C. A.; Westlake, B. C.; Paul, A.; Ess, D. H.; McCafferty, D. G.; Meyer, T. J. *Chem. Rev.* **2012**, *112*, 4016.
(41) Kuan, S. L.; Leong, W. K.; Goh, L. Y.; Webster, R. D. *Organometallics* **2005**, *24*, 4639.
(42) Pombeiro, A. J. L.; Guedes da Silva, M. F. t. C.; Lemos, M. *Coord. Chem. Rev.* **2001**, *219*, 53.

FOR TOC ONLY

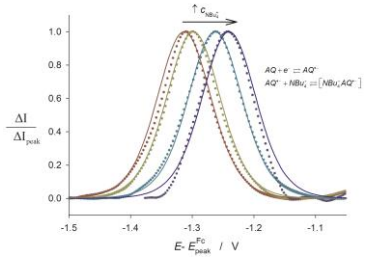
↑ $c_{NBu_4^+}$
$AQ + e^- \rightleftharpoons AQ^{\bullet-}$
$AQ^{\bullet-} + NBu_4^+ \rightleftharpoons [NBu_4AQ^{\bullet-}]^+$
$\frac{\Delta I}{\Delta I_{peak}}$
1.0
0.8
0.6
0.4
0.2
0.0
-1.5
-1.4
-1.3
-1.2
-1.1
$E - E^{Fc}_{peak}$ / V